Biogeosciences Discuss., https://doi.org/10.5194/bg-2019-4
Manuscript under review for journal Biogeosciences
Discussion started: 15 February 2019

Hyposalinity tolerance in the coccolithophorid *Emiliania huxleyi* under the influence of ocean acidification involves enhanced photosynthetic performance

Running head: Hyposalinity tolerance of *E. huxleyi* under OA

JiekaiXu[1], John Beardall[2], Kunshan Gao[1,3*]

[1]State Key Laboratory of Marine Environmental Science, College of Ocean and Earth Sciences, Xiamen University, Xiamen 361102, China

[2]School of Biological Sciences, Monash University, Clayton, VIC. 3800, Australia

[3]Laboratory for Marine Ecology and Environmental Science, Qingdao National Laboratory for Marine Science and Technology, Qingdao 266071, China

[*]Corresponding author e-mail: ksgao@xmu.edu.cn (Kunshan Gao)

Biogeosciences Discuss., https://doi.org/10.5194/bg-2019-4
Manuscript under review for journal Biogeosciences
Discussion started: 15 February 2019

Abstract

While seawater acidification induced by elevated CO_2 is known to impact coccolithophores, the effects in combination with decreased salinity caused by sea ice melting and/or hydrological events have not been documented. Here we show the combined effects of seawater acidification and reduced salinity on growth, photosynthesis and calcification of *Emiliania huxleyi* grown at 2 CO_2 concentrations (low CO_2 LC：400 μatm; high CO_2 HC：1000 μatm) and 3 levels of salinity (25, 30 and 35‰). A decrease of salinity from 35 to 25‰ increased growth rate, cell size and effective photochemical efficiency under both LC or HC. Calcification rates were relatively insensitive to combined effects of salinity and OA treatment but were highest under 35‰ and HC conditions, with higher ratios of calcification to photosynthesis (C:P) in the cells grown under 35‰ compared with those grown at 25‰. In addition, elevated dissolved inorganic carbon (DIC) concentration at the salinity of 35‰ stimulated its calcification. In contrast, photosynthetic carbon fixation increased almost linearly with decreasing salinity, regardless of the pCO_2 treatments. When subjected to short-term exposure to high light, the low-salinity-grown cells showed the highest photochemical effective quantum yield with the highest repair rate, though HC treatment enhanced PSII damage rate. Our results suggest *Emiliania huxleyi* can tolerate low salinity plus acidification conditions by up-regulating its photosynthetic performance together with a relatively insensitive calcification response, which may help it better adapt to future ocean global environmental changes, especially in the coastal areas of high latitudes.

Keywords: calcification, coccolithophore, CO_2, *Emiliania huxleyi*, ocean acidification, photosynthesis, salinity.

1 Introduction

Since the Industrial Revolution, atmospheric pCO_2 levels have increased by approximately 40%, mainly due to anthropogenic emissions of CO_2 (Howes et al., 2015), and the oceans have absorbed about one third of the fossil fuel CO_2 (Sabine et al., 2004), leading to increases in the concentration of pCO_2, HCO_3^- and H^+, along with a decrease in the concentration of CO_3^{2-} and the saturation state of calcium carbonate, a process known as Ocean Acidification (OA). The pH of surface waters of the global ocean has already decreased by 0.1 units and will be further decreased by another 0.4 units by the end of this century under a "business-as-usual" scenario (Gattuso et al., 2015).

At the same time, climate change also results in global warming, another critical issue which has an important influence on organisms, with unforeseen consequences for marine biogeochemical cycling and ecosystem functioning (Taucher and Oschlies, 2011). It is predicted that the global mean temperature will increase by 2~5 ℃ by 2100 (Gattuso et al., 2015). With warmer air and increasing ocean temperature, sea ice coverage has been declining, leading to a decrease in salinity, especially in coastal areas at high latitudes (Dickson et al., 2002; Ishii et al., 2006; Massom and Stammerjohn, 2010). Blindheim et al. (2000) and Albretsen et al. (2011) have reported a sharp decline in salinity in coastal areas of the Norwegian Sea during the

Biogeosciences Discuss., https://doi.org/10.5194/bg-2019-4
Manuscript under review for journal Biogeosciences
Discussion started: 15 February 2019

last few decades, which in some locations has been more than 0.5‰ in the last 10 years. On the other hand, rainfall or hydrological changes associated with climate change can also alter surface seawater salinity. As projected climate change processes are thought to amplify OA in the oceans of high latitude, organisms in the waters at high latitude are thought to be more vulnerable to rapid chemical changes (Chierici and Fransson, 2009; Qi et al., 2017).It is therefore of general interest to explore how marine photosynthetic organisms respond to changes in surface ocean carbonate chemistry and salinity that are potentially altered by both decreased salinity and rising CO_2 concentration.

Coccolithophores, one of the most important calcifying primary producer groups, play a key role in the global carbon cycle, contributing about 10% to total organic carbon fixation (Poulton et al., 2007) and 50% to $CaCO_3$ found in pelagic sediments (Broecker and Clark, 2009). The globally most abundant coccolithophore species is *Emiliania huxleyi*, which forms extensive blooms (Moore et al., 2012). With respect to *E. huxleyi*'s distinct sensitivity to OA, there have already been a number of studies that documented its morphological, physiological and molecular responses to OA (Paasche, 2001; Raven and Crawfurd, 2012). Riebesell et al. (2000) reported negative effects of OA on morphology, calcification and growth on *E. huxleyi,* while Iglesias-Rodriguez et al. (2008) reported higher particulate inorganic and organic carbon (PIC, POC) per cell under elevated pCO_2. Nevertheless, both studies showed decreased calcification rates under elevated pCO_2 (Riebesell et al., 2008). Hoppe et al. (2011) showed that the PIC production of two *E. huxleyi* strains was both negatively

Biogeosciences Discuss., https://doi.org/10.5194/bg-2019-4
Manuscript under review for journal Biogeosciences
Discussion started: 15 February 2019

affected by higher pCO_2, although marked differences of responses to OA did exist among strains (Langer et al., 2009). Other environmental drivers are known to interact with OA to affect *E. huxleyi* (Gao et al., 2012; Boyd et al. 2018). For instance, exposure to UV radiation or high light exacerbated impacts of OA on calcification (Feng et al., 2008; Gao et al., 2009). On the other hand, a recent study demonstrated that high levels of sunlight counteracted the negative effects of OA on calcification of *E. huxleyi* when the cells were grown under incident fluctuating solar radiation (Jin et al., 2017). Over 150 to 1000 generations, lower PIC: POC ratios were still observed in coccolithophorid species (Müller et al., 2010; Lohbeck, 2012; Tong et al. 2018). Decreased PIC:POC ratio in another coccolithophorid *Gephyrocapsa oceanica* adapted to OA over 1000 generations persisted when cells were transferred back to the low pCO_2 treatment, indicating an adaptive evolution (Tong et al. 2018). In brief, it is generally accepted that OA decreases the calcification, and discrepancies exist when OA impacts on *E. huxleyi* in combination with other factors or under multiple drivers.

Decreased salinity may interact with OA to affect *E. huxleyi*, though it is known as a euryhaline species (Birkenes et al., 1952; Paasche et al., 1996). While some *E. huxleyi* strains can survive at a salinity as low as 15‰ (Brand, 1984), its calcification is strongly depressed, with malformed coccoliths (Saruwatari et al., 2015). Observations from sediment cores also showed that coccolith morphology was dependent on salinity (Fielding et al., 2009), and salinity can affect the hydrogen isotopic composition of long chain alkenones synthesized by *E. huxleyi* (Schouten et

al., 2006). However, to the best of our knowledge, the combined effects of reduced salinity and lowered pH on *E. huxleyi* have not yet been documented, except for one investigation that addressed the combined effects of desalination and OA on a natural community of Baltic Sea pelagic microplankton dominated by the cyanobacterium *Aphanizomenon sp.* (Wulff et al., 2016). In this study, we show that *Emiliania huxleyi* can tolerate hyposalinity even when grown under OA conditions.

2 Materials and methods

2.1 Cultures and experimental setup

Emiliania huxleyi PML B92/11 was originally obtained from coastal waters off Bergen, Norway. This strain calcifies, but after having being maintained in laboratory culture for about 10 years, its calcification capacity has decreased (see Results below). Sterilized seawater was enriched with Aquil medium (Sunda et al., 2005). Monospecific cultures (without aeration) were maintained at 15℃ and illuminated by cool white fluorescent light at an intensity of 200 µmol photons m^{-2} s^{-1}, under a 12:12 h light and dark cycle. We used low biomass density batch cultures in the sealed polycarbonate bottles where *E. huxleyi* was inoculated for about 400 cells ml^{-1} at the beginning and cell concentrations were less than 60,000 cells ml^{-1} when parameters were measured so that there was no significant change of the carbonate chemistry in the culture medium (Laroche et al., 2010) and the cultures were still in the exponential phase after 4~5 days' incubation without dilution (Zondervan et al., 2002). The culture medium was equilibrated with filtered (0.22µm, Whatman) ambient air of low

(400 μatm) or elevated (1000 μatm) CO_2 concentrations prior to inoculation. We set three levels of salinity (25‰, 30‰, 35‰): 35‰ is the salinity of our artificial seawater (Harrison, 2005) and 30‰ ~ is close to the salinity of the strain's original environment (the influence of Norwegian coastal current) (Mork, 1981). The lowest level served as an extreme that is within the range of values occurring frequently in coastal and estuarine environments (Brand, 1984; Li et al., 2011). Reduced salinity was obtained by diluting prepared artificial seawater with Milli - Q water before sterilization, nutrient addition and aeration. After taking samples for carbonate chemistry measurements (see the following section), the seawater with target pCO_2 was divided carefully into three 500 ml polycarbonate bottles before inoculation. There were thus triplicate independent cultures for each treatment where the volume of each was 480 ml or so. Prior to the end of the experiment, we took samples again for carbonate chemistry measurements. Samples for measurements of physiological parameters were all taken about 2.5 h after the onset of the light period on the last day of incubation when cells grew under each treatment for about 14 generations. Before inoculation, exponential growing cells were pre-acclimated to experimental conditions for at least 7 generations, then experimental cultures were run for another 6~8 generations in the mid exponential phase with gentle shaking twice a day.

2.2 Carbonate chemistry sampling and measurements

pH was measured by a pH meter (Orion 2 STAR,Thermo Scientific) calibrated with standard National Bureau of Standards (NBS) buffers. Samples for total

Biogeosciences Discuss., https://doi.org/10.5194/bg-2019-4
Manuscript under review for journal Biogeosciences
Discussion started: 15 February 2019

alkalinity (TA) measurements were filtered (~0.7 μm), poisoned with a saturated $HgCl_2$ solution (0.5‰ final concentration), and stored at 4℃. TA was measured in triplicate (each of 3 replicate cultures) and determined by Gran acidimetric titration with a TA analyzer (AS-Alk1+, Apollo SciTech). Certified reference materials (A. Dickson, LaJolla, California) from the Scripps Institution of Oceanography were used to assure the accuracy of the TA measurement. TA and pH data were applied to CO2SYS software (Lewis et al., 1998) to calculate other carbonate chemistry parameters (Tables 1 & 2).

2.3 Specific growth rate and mean cell size determination

Cell concentration and mean cell size were measured by a Coulter Particle Count and Size Analyzer (Z2, Beckman Coulter). Specific growth rate was calculated according to the equation: $\mu = (\ln N_1 - \ln N_0) / (t_1 - t_0)$, in which N_1 and N_0 represent cell concentrations at t_1 and t_0, where t_0 represents the beginning and t_1 the end day of the cultures. The period of (t_1 - t_0) fell within the exponential growth phase as described above.

2.4 Chlorophyll and carotenoid contents

Cells for determination of pigment content were filtered onto GF/F filters (25 mm, Whatman) and then extracted overnight in absolute methanol at 4℃ in darkness (Li et al. 2017). After centrifugation (5000 g for 10 min), the absorption values of the sample supernatants were analyzed by a UV–VIS spectrophotometer (DU800,

Biogeosciences Discuss., https://doi.org/10.5194/bg-2019-4
Manuscript under review for journal Biogeosciences
Discussion started: 15 February 2019

Beckman Coulter). The concentrations of chlorophylls *a* and *c* were calculated according to (Ritchie, 2006):

Chl *a* ($\mu g\ ml^{-1}$) = 13.2654* ($A_{665} - A_{750}$) – 2.6839 * ($A_{632} - A_{750}$);

Chl *c* ($\mu g\ ml^{-1}$) = -6.0138 *($A_{665} - A_{750}$) + 28.8191* ($A_{632} - A_{750}$).

Carotenoid concentration was determined by the equation given by Strickland and Parsons (1972):

Carotenoid ($\mu g\ ml^{-1}$) = 7.6 *(($A_{480} - A_{750}$) – 1.49 * ($A_{510} - A_{750}$));

where A_x indicates the absorbance at a wavelength x. The pigment content per cell was calculated by taking the dilution factor and cell concentration into account.

2.5 Chlorophyll *a* fluorescence

The photochemical parameters were determined using a Multiple Excitation Wavelengths Chlorophyll Fluorescence Analyzer (Multi-color-PAM, Walz). Maximum and effective photochemical quantum yields were determined according to the equations of Genty et al. (1989): maximum photochemical quantum yield (F_v / F_m) = (F_m - F_0) / F_m , for dark-adapted (10 min) samples; effective photochemical quantum yield Φ_{PSII} (F'_v / F'_m) = ($F'_m - F_t$) / F'_m for light-adapted samples, where F_m and F'_m indicate maximum chlorophyll fluorescence of dark and growth-light-adapted samples, respectively; F_0 is the minimum chlorophyll fluorescence of dark-treated cells; and F_t is the steady-state chlorophyll fluorescence of light exposed samples. Φ_{PSII} was measured under actinic light intensity (~240 µmol photons $m^{-2}\ s^{-1}$) similar to the culture light level. The saturation pulse was set at 5000 µmol photons $m^{-2}\ s^{-1}$, and

Biogeosciences Discuss., https://doi.org/10.5194/bg-2019-4
Manuscript under review for journal Biogeosciences
Discussion started: 15 February 2019

lasted for 0.8 s.

Another experiment was carried out on the last day of incubations, investigating the response of cells under each treatment to high light exposure. Samples were placed in 35 ml quartz tubes wrapped with Ultraphan film 395 (UV Opak, Digefra), receiving irradiances above 395 nm (PAR). The transmission details of this cut-off foil and quartz tubes are available elsewhere (Gao et al., 2007). The tubes for fluorescence measurements were placed under a solar simulator (Sol 1200W; Dr. Hönle, Martinsried, Germany). The cells were exposed to PAR of 800 µmol photons m^{-2} s^{-1} for 48 min at 15℃ (growth temperature) while maintaining the tubes in a circulating water bath for temperature control (CTP-3000, Eyela). During the exposures, measurements of fluorescence parameters were carried out (see above). Aliquots of 2.5 ml of sample from each tube (total of 18 tubes, that is, triplicate per each treatment) were taken every 3-10 min during exposure, and immediately measured (without any dark adaptation) to get the instant maximum fluorescence F'_m and the steady state fluorescence F_t of the light adapted cells, and Φ_{PSII} was calculated as described above. The rates of high light-induced damage to PSII (k, min^{-1}) and the corresponding repair rates (r, min^{-1}) were estimated according to Beardall et al. (2014), applying the Kok model that assumes simultaneous operation of the damage and recovery during the photoinhibitory exposures, and calculated as follows: ,:

$$P_n/P_0 = r / (r + k) + k / (r+k)*\exp(-(r + k) *t);$$

where P_n and P_0 represent effective quantum yield values at time t (minutes) and time zero, respectively.

Biogeosciences Discuss., https://doi.org/10.5194/bg-2019-4
Manuscript under review for journal Biogeosciences
Discussion started: 15 February 2019

214 **2.6 Determination of photosynthetic and calcification rates**

215 On the last day of the cultures, the cells were collected in the middle of the
216 photoperiod, dispensed into borosilicate bottles (20 ml) and inoculated with 5 μCi
217 (0.185 MBq) of labelled sodium bicarbonate (Amersham). After 2 h of incubation
218 under the same environment as the cultures, samples were immediately filtered under
219 dim light onto Whatman GF/F glass fiber filters (25 mm), rinsed with unlabeled
220 medium, placed in 20 mL scintillation vials, and then dried (60℃, 5 h) before
221 counting in a liquid scintillation counter (Beckman, LS6500) with 5 ml scintillation
222 cocktail (Perkin Elmer). In parallel, another filter with the cells was fumed with HCl
223 overnight to expel non-fixed ^{14}C for measurement of photosynthetic ^{14}C fixation. The
224 rate of calcification of *E. huxleyi* was estimated as the difference between the total and
225 the photosynthetic carbon fixation (Paasche, 1963; Gao et al., 2009). Two samples for
226 calcification (30‰ HC，35‰ LC) were lost during measurements, so are not reported
227 in the results.

228 **2.7 Statistical analyses**

229 Data were analyzed by using SPSS software. Before performing parametric tests,
230 data were tested for homogeneity of variance (Levene test) and normality (Shapiro -
231 Wilk test). The two-way ANOVA with pCO_2 (two levels) and salinity (three levels)
232 classed as factors in the model was used at a significance level of $p < 0.05$. When p
233 value was under 0.05, the post hoc Duncan test was used to determine differences
234 between treatments. Data were reported as mean ± SD.

235

Biogeosciences Discuss., https://doi.org/10.5194/bg-2019-4
Manuscript under review for journal Biogeosciences
Discussion started: 15 February 2019

3 Results

3.1 Specific growth rate and cell size

No interactive effects were found, but individual effects of salinity and pCO_2 were observed (two-way ANOVA, $F_{(2,12)} = 1.580$, $p = 0.246$; salinity $F_{(2,12)} = 5.574$, $p = 0.019$; pCO_2 $F_{(1,12)} = 66.545$, $p < 0.001$).

There were significant differences in growth rate between 25‰ and 35‰ (one-way ANOVA, $p < 0.05$) under both LC and HC with significant differences also found between 30‰ and 35‰ under LC (one-way ANOVA, $p = 0.022$), while no significant difference was found in growth rate between 25‰ and 30‰ (Fig. 1a, one-way ANOVA, $p = 0.434$, $p = 0.053$). Under LC, compared to 35‰, treatments with salinity levels of 25‰ or 30‰ enhanced growth rate by 10% ($p = 0.009$) and 8% ($p = 0.022$), respectively. Under HC, 25‰ and 30‰ enhanced growth rate by 9% ($p = 0.037$) and 10% ($p = 0.103$). For all salinity treatments, OA treatment decreased the growth rate by 19% ($p = 0.001$), 16% ($p = 0.020$) and 18% ($p = 0.003$) compared to that of LC-grown cells under 25‰, 30‰ and 35‰, respectively.

Cell size ranged from 4.20 μm to 4.88 μm. Mean cell sizes were largest in the 25‰ treatment and smallest at 30‰ under both LC and HC (Fig. 1b). OA decreased cell size under all salinity treatments.

3.2 Pigment content

Significant interaction effects and effects of salinity and pCO_2, respectively on chlorophyll *a* content of cells were observed (two-way ANOVA, $F_{(2,12)} = 55.102$, $p <$

Biogeosciences Discuss., https://doi.org/10.5194/bg-2019-4
Manuscript under review for journal Biogeosciences
Discussion started: 15 February 2019

0.001; salinity $F_{(2,12)} = 42.433$, $p < 0.001$; pCO_2 $F_{(1,12)} = 48.006$, $p < 0.001$). Growth at 25‰ increased chlorophyll *a* content of cells, which was 72% ($p < 0.001$) higher than at 30‰ and 1.8 times higher ($p < 0.001$) than at 35‰ under HC (Fig. 2a). Under LC, there were no significant differences between 25‰ and 35‰ (one-way ANOVA, $p = 0.698$), 30‰ and 35‰ (one-way ANOVA, $p = 0.055$) while 30‰ increased the chlorophyll *a* content of cells by 19% ($p = 0.032$) relative to 25‰. In the 25‰ treatment, HC increased the chlorophyll *a* content of cells by 28% ($p = 0.040$) relative to that of LC cells. However, chlorophyll *a* content was higher in the LC treatment than HC under both 30‰ and 35‰. LC increased chlorophyll *a* content by 60% ($p < 0.001$) compared to HC under 30‰ and it was 1.28 times higher ($p < 0.001$) than in the HC treatment under 35‰.

The trend of carotenoid content of cells was same as for chlorophyll *a* (Fig. 2c) that the value was higher in the LC treatment than at HC under 30‰ and 35‰, although there was no significant difference between LC and HC under 25‰ (one-way ANOVA, $p = 0.144$). There were also no significant differences among the three salinity treatments under LC (one-way ANOVA, $F_{(2,6)} = 1.620$, $p = 0.274$). Under HC, the carotenoid content increased at the low salinity, by 43% ($p < 0.001$) and 1.39 times ($p < 0.001$) in the 25‰ treatment relative to 30‰ and 35‰, respectively.

There were significant differences between cells grown at 25‰ and 35‰, and between 30‰ and 35‰ for chlorophyll *c* content under both LC (one-way ANOVA, $p = 0.011$, $p = 0.005$) and HC (one-way ANOVA, $p < 0.001$), while no significant difference was found between cells grown at 25‰ and 30‰ (Fig. 2b, one-way

Biogeosciences Discuss., https://doi.org/10.5194/bg-2019-4
Manuscript under review for journal Biogeosciences
Discussion started: 15 February 2019

ANOVA, p = 0.420, p = 0.212). Among the three salinity levels, only in the 35‰ treatment could a higher chlorophyll *c* content under LC than HC be observed.

3.3 Chlorophyll *a* fluorescence

The maximal photochemical quantum yields varied little among all treatments, ranging from 0.53 ± 0.01 to 0.55 ± 0.02 (Fig. 3a). Elevated pCO_2 scarcely influenced effective photochemical quantum yields under all salinity treatments (Fig. 3b). The only exception was that Φ_{PSII} in HC cells decreased by 17% (p = 0.001) relative to that of LC cells under 25‰. Under LC, 25‰ stimulated Φ_{PSII} by 31% (p = 0.003) and 17% (p = 0.026) compared to cells in 30‰ and 35‰, respectively. Under HC, there was a significant difference only between cells at 25‰ and 35‰ (one-way ANOVA, p < 0.05) among the three salinity treatments, where growth at 25‰ increased Φ_{PSII} by 13% (p = 0.039) relative to the 35‰ treatment (Fig. 3b).

3.4 Photosynthesis and calcification

Regardless of pCO_2 levels, photosynthetic carbon fixation decreased with increasing salinity (Fig. 4a). Cells grown under 25‰ had a photosynthesis rate 1.8 times higher than in 35‰ under LC (one-way ANOVA, p < 0.001) and 2.7 times higher (p < 0.001) than under HC. OA generally decreased photosynthetic carbon fixation with the only exception being that no significant difference was found between LC and HC under 30‰ (one-way ANOVA, p = 0.158) although the mean value of the former was still 30% higher (Fig. 4a).

Biogeosciences Discuss., https://doi.org/10.5194/bg-2019-4
Manuscript under review for journal Biogeosciences
Discussion started: 15 February 2019

The calcification rates ranged from 0.03 ± 0.01 to 0.08 ± 0.02 pg C cell^{-1} h^{-1}. No significant differences were found among all salinity treatments under LC (one-way ANOVA, $F_{(2,5)} = 1.775$, $p = 0.262$). In contrast, growth at 35‰ stimulated the calcification rates of cells by 75% ($p = 0.042$) and by 1.3 times ($p = 0.013$) compared to values in cells grown at 25‰ and 30‰, respectively under HC. An effect of OA was not found under the 35‰ treatment while it decreased calcification rates by 50% under 25‰ ($p = 0.044$) and 30‰, although there were no significant differences between LC and HC under the 30‰ treatment (one-way ANOVA, $p = 0.170$). No significant interaction effects of salinity and pCO_2 on the calcification rates were found, though individual effects of salinity and pCO_2 were significant (two-way ANOVA, $F_{(2,10)} = 3.621$, $p = 0.066$; salinity $F_{(2,10)} = 4.138$, $p = 0.049$; pCO_2 $F_{(1,10)} = 7.977$, $p = 0.018$).

Significant interaction effects and individual effects of salinity and pCO_2 were found in the ratio of calcification (C) to photosynthesis (P) (two-way ANOVA, $F_{(2,10)} = 11.286$, $p = 0.003$; salinity $F_{(2,10)} = 37.050$, $p < 0.001$; pCO_2 $F_{(1,10)} = 5.028$, $p = 0.049$). Seawater acidification and high salinity acted synergistically to stimulate the C:P ratio, thus resulting in the highest value under the 35‰ HC treatment. Salinity seemed to play a more important role as no significant differences between LC and HC were found with the only exception being under 35‰ where OA increased the ratio by 103% ($p = 0.027$). With increasing salinity, the C:P ratio increased regardless of pCO_2 levels. Under LC, the C:P value of cells grown under 35‰ was 1.2 times ($p = 0.044$) and 70% higher ($p = 0.108$) than at 25‰ and 30‰ respectively, with the

Biogeosciences Discuss., https://doi.org/10.5194/bg-2019-4
Manuscript under review for journal Biogeosciences
Discussion started: 15 February 2019

equivalent values being 4.9 times (p = 0.001) and 3.9 times (p = 0.001) higher under HC.

3.5 Photochemical responses

When exposed to high light (800μmol photons m^{-2} s^{-1}), the effective photochemical quantum yield Φ_{PSII} decreased significantly during the first 0–15 min of exposure in all salinity/pCO_2 treatments (Fig. 5); after this period, Φ_{PSII} remained more or less constant. Regardless of pCO_2 levels, the samples grown under 25‰ had a smaller decrease in Φ_{PSII}.

This trend was especially clear under LC (Fig. 5a). During the whole exposure process, the Φ_{PSII} value of the cells under the 25‰ treatment was highest, with the lowest value reached being ca. 0.21 after 48 min exposure, which was 4.4 (one-way ANOVA, p = 0.004) and 80% (p = 0.045) higher than that of cells from 30‰ and 35‰ treatments, respectively. In contrast, Φ_{PSII} of the 30‰ treatment was always lowest during the whole exposure process.

In the HC-grown cells, Φ_{PSII} declined much faster compared to that in the LC-grown cells except that at some time points, the value of Φ_{PSII} was higher in HC-grown cells under the 30‰ treatment (Fig. 5b). No significant differences in Φ_{PSII} among three salinity treatments were found during the whole exposure (Fig. 5b). The only exception was that the 25‰ treatment showed higher values of Φ_{PSII} by 131% (one-way ANOVA, p = 0.033) and 108% (p = 0.060), respectively, relative to that of the 30‰ and 35‰ treatments at 6 min from the start of the exposure. Nonetheless,

346 Φ_{PSII} of the 25‰ treatment was still highest during the whole exposure process, with
347 the lowest value reached being ca. 0.1.

348 After cells were exposed to short-term, acute exposures to elevated levels of
349 visible solar radiation, there was a significant difference in repair rates among the
350 three salinity treatments under LC (Fig. 6a). The highest *r* values were observed under
351 the 25‰ treatment, which were 4.5 times (one-way ANOVA, $p = 0.007$) and 83%
352 higher ($p = 0.045$) than those of 30‰ and 35‰ treatments while no significant
353 differences were observed under HC ($p = 0.141$). No significant differences in
354 damage rates were observed under HC among three salinity treatments ($p = 0.122$)
355 (Fig. 6b). While under LC, *k* values was highest in the 30‰ treatment and reached
356 about 0.4 min^{-1}, a value which was 1.4 times ($p = 0.001$) and 90% higher ($p = 0.003$)
357 than those of 30‰ and 35‰ treatments, respectively.

358 From the ratio of *r*/*k*, it is clear that under LC, cells grown at the salinity of 25‰
359 showed the best ability to cope with the high light stress but appeared to do worst
360 under 30‰ (Fig. 6c). In contrast, the performance of cells grown under different
361 salinity treatments showed no significant differences under HC ($p = 0.392$).

362

363 **4 Discussion**

364 Large populations of *E. huxleyi* are observed every summer in Norwegian coastal
365 waters (Holligan et al., 1993; Wal et al., 1995). Considering that *E. huxleyi* is an
366 essentially oceanic species with an offshore center of distribution (Winter et al., 1994),
367 its success in Norwegian coastal waters is noteworthy. Paasche et al. (1996) inferred

368 that *E. huxleyi* may have developed distinct ecotypes in Scandinavian coastal waters.
369 By coincidence, the strain in our study (PML B92/11) was originally obtained from
370 coastal waters off Bergen, Norway. Here, although we cannot provide genetic data,
371 instead we focus on its physiological performance under changing levels of salinity
372 (25‰ ~ 35‰) and carbonate chemistry induced with elevated CO_2 (1000 µatm). We
373 found that a reduction in salinity to 25‰ increased growth rate, effective
374 photochemical efficiency and photosynthetic carbon fixation even under ocean
375 acidification (OA) conditions, and its calcification rates were highest under 35‰ and
376 OA conditions. The tolerance of reduced salinity under OA could be attributed to its
377 increased light capturing capability due to increased cellular photosynthetic pigments
378 and enhanced light use efficiency and photo-repair in photosystem II. Discussion in
379 details are as follows:

380 *E. huxleyi* (PML B92/11) cells had a higher growth rate under reduced salinity
381 (25‰) when grown under ambient level of pCO_2 (LC, Fig. 1a). This result is
382 consistent with previous studies (Brand, 1984; Schouten et al., 2006), showing that
383 strains isolated from coastal regions grew more rapidly under 25‰ than 33‰. Brand
384 (1984) suggested that the last deglaciation was a possible selection time for coastal
385 populations adapted for lower salinity. In the present study, since big differences in
386 seawater carbonate chemistry exist between 25‰ and 35‰ (Table 2), increased CO_2
387 availability by about 39% might be the key reason (Fig. 1).

388 Strains that have different calcifying capacities have different DIC transport
389 abilities (Elzenga et al., 2000; Paasche, 2001). After a long time in laboratory culture,

390 the capacity to calcify of the strain used in this work has declined: the value of
391 calcification rates (0.03 ± 0.01 to 0.08 ± 0.02 pg C $cell^{-1}$ h^{-1}) determined here is lower
392 compared to the values of 0.29-0.46 pg C $cell^{-1}$ h^{-1} reported by another study with the
393 same strain used (Sett et al., 2014). It's reported that low–calcifying strains are less
394 efficient in utilizing bicarbonate for assimilation (Nimer and Merrett, 1992; Rost et al.,
395 2003). Thus, growth of this strain might largely rely on the availability of CO_2. At 25‰
396 in the present work, cells' growth was increased by 9-10% as there was more
397 dissolved CO_2 in cultures compared to treatments under 30‰ and 35‰. Although
398 enhanced growth rate of *E. huxleyi* (NZEH, AC472 and NIES 837) under elevated
399 CO_2 concentrations has been reported before (Shi et al., 2009; Fiorini et al., 2011;
400 Fukuda et al. 2014), in the present study, the growth of *E. huxleyi* was lowered by
401 16-19% under HC condition regardless of the salinity levels compared to LC-grown
402 cells, which suggests that increased acidity under OA could have stressed the cells
403 (Fig. 1a). Seawater acidification as a result of increased pCO_2 has also been shown to
404 inhibit growth rate of *E. huxleyi* in other studies (Nimer et al., 1994; Hoppe et al.,
405 2011).

406 The photosynthetic rates, in accordance with the growth rate, increased with
407 decreased salinity under both LC and HC (Fig. 4a). Such a relationship in
408 photosynthesis was more obvious than in the specific growth rate (Figs 1&4). Since
409 mitochondrial respiration rate of *E. huxleyi* is enhanced under elevated CO_2
410 concentrations (Jin et al., 2015), the balance between photosynthesis and respiration
411 can reasonably be reflected in the growth response (Fig. 1a). The complexities of

Biogeosciences Discuss., https://doi.org/10.5194/bg-2019-4
Manuscript under review for journal Biogeosciences
Discussion started: 15 February 2019

412 inorganic carbon use of *E. huxleyi,* especially in relation to which species of inorganic
413 carbon (CO_2 or HCO_3^- or both) is the primary source for photosynthesis, remain
414 controversial (Sekino et al., 1994; Bach et al., 2011; Monteiro et al., 2016). Recently,
415 CO_2 has been suggested to be the main inorganic carbon source for photosynthesis in
416 calcifying strains of *E. huxleyi* (Bach et al., 2013; Stojkovic et al., 2013). Therefore,
417 reduced salinity with the increased availability of CO_2 would have resulted in higher
418 photosynthetic rates. In this study, cells grown under 25‰ exhibited photosynthesis
419 rates about 2 times higher than in 35‰ (Fig. 4a), while differences of [CO_2] between
420 25‰ and 35‰ media were much smaller (Table 2). The reason behind this can be
421 associated with the function of CCMs, which makes the discrepancies in intracellular
422 [CO_2] far larger than those of the surrounding medium (Rost et al., 2003; Schulz et al.,
423 2007), although the CCMs of *E. huxleyi* are supposed to be low (Rost and Riebesell,
424 2004). Furthermore, a higher photosynthesis under reduced salinity (25‰ and 30‰)
425 implies the process of osmoregulation that the cells need to release more organic
426 osmolytes into the medium to cope with hypo-osmotic stress, as many organic
427 osmolytes are typically photosynthetic products (Kirst, 1990).

428 In our study, cells grown under HC conditions had lower photosynthesis rates
429 irrespective of salinity treatments (Fig 4a). The negative effects of low pH ($\leqslant$ 7.7)
430 could have offset the positive effects of increasing [CO_2] (about twice that of LC
431 medium, Table 2) as previous studies show that higher intracellular [H^+] would
432 directly result in a decreased pH in the stroma of the chloroplast, which then led to
433 reduced CO_2 fixation (Werdan et al., 1975; Coleman et al., 1981; Suffrian et al., 2011).

In addition, HC treatment might down-regulate the efficiency of CCMs, thus resulting in lower intracellular [CO_2] and reduced photosynthetic rate compared to LC, as reflected in a diatom (Liu et al. 2017).

Calcification rates of *E. huxleyi* are known to be sensitive to changes in seawater carbonate chemistry. As HCO_3^- is the main substrate for calcification (Buitenhuis et al., 1999; Paasche, 2001), the increasing calcification rates of cells grown under HC with increasing salinity in our study (Fig. 4b) could be the result of increased [HCO_3^-] concentration (Tables 1&2). However, there were no significant differences in calcification rates among three salinity treatments under LC with even a slightly higher value at 25‰ (Fig. 4b), which is consistent with Beaufort et al. (2011), who also showed weak correlation between calcification and salinity. Under LC, the highest effective photochemical quantum yield values and *r*:*k* ratios were observed under 25‰ among the three salinity treatments after an exposure to high light (Figs. 5a & 6c), suggesting a relative thick coccolith layer (Xu and Gao, 2012), which was in accordance with the ^{14}C results as described above (Fig. 4b). Nimer and Merrett (1993) proposed that the optimum pH for calcification was 7.8, a value just close to the pH of our medium under 25‰ and LC condition (Table 2), although the strains they used were different from that in our study. Sikes and Wilbur (1982) demonstrated that, when salinity was reduced from 34.5‰ to 19.5‰, the percentage of calcified cells increased in the medium. Therefore, the existence of a coccosphere may help to regulate osmotic pressure and impart on cells a greater tolerance to low salinity, which could partially explain the abundant coccoliths found in the sloped sediments of

Biogeosciences Discuss., https://doi.org/10.5194/bg-2019-4
Manuscript under review for journal Biogeosciences
Discussion started: 15 February 2019

456 Mississippi continental shelf (Doyle and Sparks, 1980) and the burst of
457 coccolithophore blooms in the Gulf of Mexico with a large amount of freshwater
458 input from the Mississippi River (O'Connor et al., 2016). Taylor et al. (2011)
459 identified a plasma membrane H^+ channel that played an important role in pH
460 homeostasis in coccolithophores. Both rectifying H^+ channels and rectifying Cl^-
461 channels worked together to sustain H^+ efflux. In our study, the lower concentration of
462 Cl^- associated with the reduced salinity in the 25‰ medium implies that Cl^- efflux
463 was easier to carry out and assist H^+ removal to keep the intracellular pH stable,
464 which could ultimately have promoted calcification.

465 We also found that the difference in calcification rate between LC and HC cells
466 gradually reversed with increasing salinity (Fig. 4b). Calcification rates of *E. huxleyi*
467 (PMLB 92/11) at high pCO_2 appeared to be dependent on pH (Bach et al., 2011).
468 Indeed, we suggest such reversal was due to changes in the proportion of [HCO_3^-]
469 and pH in the milieu. Specifically, calcification would generate quantities of H^+ that
470 must be rapidly removed to prevent cytoplasmic acidification. Under LC, it was easier
471 for the cells to remove H^+ (Mackinder et al., 2010), while under HC the concentration
472 of [HCO_3^-], the substrate (bicarbonate ions) for calcification, was higher (Tables 1 &
473 2). The proportion of [HCO_3^-] in terms of total inorganic carbon increased with
474 increasing salinity (Table 2) and thus led to a slightly higher calcification rate under
475 35‰ and HC conditions (Fig. 4b), which is consistent with the result reported by
476 Fukuda et al. (2014). This finding helped to enhance our understanding as to why
477 coccolithophores were able to thrive in the early Mesozoic era, a time that was

478 characterized by relatively low sea water pH (as low as pH 7.7) and high DIC
479 concentrations (Ridgwell, 2005).

480 Cell diameters of *E. huxleyi* measured here are a combination of both the
481 thickness of the coccolith layer and the size of protoplast. The highest value of the cell
482 diameter under LC was observed in 25‰ treatment (Fig. 1b), which was because the
483 cells grown at salinity 25‰ had the highest photosynthesis rate and a relatively high
484 calcification rate (Figs. 4a & 4b). As for the smaller diameters at salinity 35‰, this
485 could be a result of a more pronounced decrease in organic carbon fixation than the
486 increase in calcification along with increased salinity (Fig. 4a & 4b).

487 From the ratio of calcification to photosynthesis (C:P), we could see different
488 strategies cells adopted when they grew under different carbonate chemistry
489 conditions. A quite low value for this parameter (< 0.2) under 25‰ and 30‰
490 regardless of pCO_2 (Fig. 4c) indicates that organic carbon production was prioritized
491 over inorganic carbon production at the DIC levels. In contrast, the C:P ratio was far
492 higher (> 0.3) under 35‰ (Fig. 4c), suggesting that cells would "invest" more
493 inorganic carbon to secrete coccoliths if the DIC supply was increased (Tables 1 & 2).
494 The results of an additional experiment (for details see supplementary materials)
495 clearly provided evidence for such behavior: when the salinity was set at 25‰ with
496 elevated DIC concentration, its C:P ratio significantly increased (Fig. S1). This result
497 agreed with previous findings (Bach et al., 2013) with qRT-PCR analysis, showing
498 that some genes with putative roles in DIC, Ca^{2+} and H^+ transport (*AEL1, CAX3* and
499 *ATPVc'/c*) may play a dual role, supporting calcification under ambient conditions but

switching to support photosynthesis when DIC becomes limiting.

Our results suggest that *E. huxleyi* PML B92/11 has the ability to acclimate to different levels of salinity + pCO_2, explaining its success in coastal waters, an environment characterized by acute changes in pCO_2 and salinity. Tyrrell et al. (2007) reported that *E. huxleyi* could only survive in natural waters with salinity above 11. We found that when salinity was further decreased to 15‰, cells of this strain could hardly survive, with non-measurable growth (data not shown). Since sensitivity of different strains of *E. huxleyi* to ocean acidification differs substantially (Langer et al. 2009), combined effects of OA and salinity would therefore be different in different regieons or under different hydrological processes.

Under the future scenario of ocean acidification with decreased salinity, the tolerance ability of *E. huxleyi* showed in this study will increase its competitiveness and help it better adapt to future global environmental changes, especially in the coastal areas of high latitude. A potential niche extension of *E. huxleyi* then would influence the distribution of other phytoplankton and have profound consequences for the ocean's carbon cycle. Thus, further studies that could better mimic the future scenario are needed.

Acknowledgements

We would like to thank Dr. John Beardall for his advice on the manuscript. This study was supported by the National Natural Science Foundation (41430967, 41720104005), and the NSFC - Shandong Joint Fund for Marine Ecology and Environmental

522 Sciences (No. U1606404). We are grateful to Liping Wu and Xiaowen Jiang for their
523 help with the experiments.

References

Albretsen, J., Aure, J., Sætre, R., and Danielssen, D. S.: Climatic variability in the Skagerrak and coastal waters of Norway, ICES J Mar Sci., 69, 758-763, doi: 10.1093/icesjms/fsr187, 2011.

Bach, L. T., Riebesell, U., and Schulz, K. G.: Distinguishing between the effects of ocean acidification and ocean carbonation in the coccolithophore *Emiliania huxleyi*, *Limnol.* Oceanogr., 56, 2040-2050, doi: 10.4319/lo.2011.56.6.2040, 2011.

Bach, L. T., Mackinder, L. C., Schulz, K. G., Wheeler, G., Schroeder, D. C., and Brownlee, C., et al.: Dissecting the impact of CO_2 and pH on the mechanisms of photosynthesis and calcification in the coccolithophore *Emiliania huxleyi*, New Phytol., **199**, 121-34, doi: 10.1111/nph.12225, 2013.

Beaufort, L., Probert, I., De, G. T., Bendif, E. M., Ruizpino, D., and Metzl, N., et al.: Sensitivity of coccolithophores to carbonate chemistry and ocean acidification, Nature **476**, 80-3. doi: 10.1038/nature10295, 2011.

Beardall, J., Stojkovic, S., and Gao, K.: Interactive effects of nutrient supply and other environmental factors on the sensitivity of marine primary producers to ultraviolet radiation: implications for the impacts of global change, Aquat Biol., **22**, 5-23, doi: 10.3354/ab00582, 2014.

Birkenes, E., and Braarud, T.: Phytoplankton in the Oslo Fjord during a '*Coccolithus huxleyi*-summer'. Avh. norske Vidensk. *Akad. Mat.-Nat. Kl*, *2*, 1952.

Blindheim, J., Borovkov, V., Hansen, B., Malmberg, S. A., Turrell, W. R., and

546 Østerhus, S.: Upper layer cooling and freshening in the Norwegian sea in relation
547 to atmospheric forcing, Deep-Sea Res. I **47**, 655-680, doi:
548 10.1016/S0967-0637(99)00070-9, 2000.
549 Boyd PW, Collins S, Dupont S, et al : Experimental strategies to assess the biological
550 ramifications of multiple drivers of global ocean change—A review, Glob
551 Change Biol., 24, 2239–2261. doi:10.1111/gcb.14102, 2018.
552 Brand, L. E.: The salinity tolerance of forty-six marine phytoplankton isolates,
553 Estuarine, Coastal Shelf Sci. **18**, 543-556. doi: 10.1016/0272-7714(84)90089
554 -1,1984.
555 Broecker, W., and Clark, E.: Ratio of coccolith $CaCO_3$ to foraminifera $CaCO_3$ in late
556 Holocene deep sea sediments, Paleoceanography **24**, 235-236, doi:
557 10.1029/2009PA00173, 2009.
558 Buitenhuis, E. T., Baar, H. J. W. D., and Veldhuis, M. J. W.: Photosynthesis and
559 calcification by *Emiliania huxleyi* (Prymnesiophyceae) as a function of inorganic
560 carbon species, J. Phycol., **35**, 949-959. doi:
561 10.1046/j.1529-8817.1999.3550949.x, 1999.
562 Chierici, M., & Fransson, A.: Calcium carbonate saturation in the surface water of the
563 Arctic ocean: undersaturation in freshwater influenced shelves, Biogeosciences **6**,
564 2421-2431, doi: 10.5194/bg-6-2421-2009, 2009.
565 Coleman, J. R., & Colman, B.: Inorganic carbon accumulation and photosynthesis in a
566 blue-green alga as a function of external pH, *Plant Physiol.,* **67**, 917-921. doi:
567 10.1104/pp.67.5.917, 1981.

568 Dickson, B., Yashayaev, I., Meincke, J., Turrell, B., Dye, S., and Holfort, J.: Rapid
569 freshening of the deep North Atlantic ocean over the past four decades, Nature
570 **416**: 832-837, doi: 10.1038/416832a, 2002.
571 Doyle, L. J., and Sparks, T. N.: Sediments of the Mississippi, Alabama, and Florida
572 (MAFLA) continental shelf, J Sediment Res., **50**, 905-195,
573 doi:10.1306/212F7B1C-2B24-11D7-8648000102C1865D, 1980.
574 Elzenga, J. T. M., Prins, H., & Stefels, J.: The role of extracellular carbonic anhydrase
575 activity in inorganic carbon utilization of *Phaeocystis globosa*
576 (Prymnesiophyceae): a comparison with other marine algae using the isotopic
577 disequilibrium technique, Limnol. Oceanogr., **45**, 372-380, doi:
578 10.4319/lo.2000.45.2.0372, 2000.
579 Feng, Y., Warner, M. E., Zhang, Y., Sun, J., Fu, F. X., Rose, J. M., et al.: Interactive
580 effects of increased pCO_2, temperature and irradiance on the marine
581 coccolithophore *Emiliania huxleyi* (Prymnesiophyceae), *Eur. J. Phycol.,* **43**,
582 87-98. doi:10.1080/09670260701664674, 2008.
583 Fielding, S. R., Herrle, J. O., Bollmann, J., Worden, R. H., and Montagnesd, D. J. S.:
584 Assessing the applicability of *Emiliania huxleyi* coccolith morphology as a
585 sea-surface salinity proxy, Limnol. Oceanogr., **54**, 1475-1480, doi:
586 10.4319/lo.2009.54.5.1475, 2009.
587 Fiorini, S., Middelburg, J. J., and Gattuso, J. P.: Testing the effects of elevated pCO_2
588 on coccolithophores (Prymnesiophyceae): comparison between haploid and
589 diploid life stages, *J. Phycol.,* **47**, 1281-1291. doi:

10.1111/j.1529-8817.2011.01080.x, 2011.

Fukuda, S. Y., Suzuki, Y., and Shiraiwa, Y.: Difference in physiological responses of growth, photosynthesis and calcification of the coccolithophore *Emiliania huxleyi* to acidification by acid and CO_2 enrichment, Photosynth Res., **121**, 299-309. doi:10.1007/s11120-014-9976-9, 2014.

Gao, K., Guan, W., and Helbling, E. W.: Effects of solar ultraviolet radiation on photosynthesis of the marine red tide alga *Heterosigma akashiwo* (Raphidophyceae), Photochem. Photobiol., **86**, 140-148. doi: 10.1016/j.jphotobiol.2006.05.007,2007.

Gao, K., Ruan, Z., Villafañe, V. E., Gattuso, J. P., and Helbling, E. W.: Ocean acidification exacerbates the effect of UV radiation on the calcifying phytoplankter *Emiliania huxleyi*, Limnol. Oceanogr., **54**,1855–1862, doi: 10.4319/lo.2009.54.6.1855, 2009.

Gao, K., Helbling, E. W., D-P, H., and Hutchins, D. A.: Responses of marine primary producers to interactions between ocean acidification, solar radiation, and warming, Mar. Ecol. Prog. Ser., **470**, 167-189, doi: 10.3354/meps10043, 2012.

Gattuso, J. P., Magnan, A., Billé, R., Cheung, W. W., Howes, E. L., and Joos, F., et al.: Contrasting futures for ocean and society from different anthropogenic CO_2 emissions scenarios, Science **349**, aac4722, doi: 10.1126/science.aac4722, 2015.

Genty, B., Briantais, J. M., and Baker, N. R.: The relationship between the quantum yield of photosynthetic electron transport and quenching of chlorophyll fluorescence, Biochim. Biophys. Acta **990**, 87-92, doi:

10.1016/S0304-4165(89)80016-9, 1989.

Harrison, P. J. and J.A. Berges.: "Marine Culture Media," In Algal Culturing Techniques. R. Andersen (Academic Press), 21-34, 2005.

Holligan, P. M., Groom, S. B., & Harbour, D. S.: What controls the distribution of the coccolithophore, *Emiliania huxleyi*, in the North sea?, Fish. Oceanogr., **2**, 175–183. doi: 10.1111/j.1365-2419.1993.tb00133.x, 1993.

Hoppe, C. J. M., Langer, G., and Rost, B.: *Emiliania huxleyi*, shows identical responses to elevated pCO_2 in TA and DIC manipulations, Journal of Experimental Mar. Biol., **406**, 54-62. doi: 10.1016/j.jembe.2011.06.008, 2011.

Howes, E., Joos, F., Eakin, C. M., and Gattuso, J. P.: An updated synthesis of the observed and projected impacts of climate change on the chemical, physical and biological processes in the oceans, Fron Mari Sci., **2**, *36*, doi: 10.3389/fmars.2015.00036, 2015.

Iglesias-Rodriguez, M. D., Halloran, P. R., Rickaby, R. E. M., Hall, I. R., Colmenero-Hidalgo, E., and Gittins, J. R., et al.: Phytoplankton Calcification in a High-CO_2 world, Science **320**, 336-340, doi: 10.1126/science.1154122, 2008.

Ishii, M., Kimoto, M., Sakamoto, K., and Iwasaki, S. I.: Steric sea level changes estimated from historical ocean subsurface temperature and salinity analyses, J. Oceanogr **62**, 155-170. doi: 10.1007/s10872-006-0041-y, 2006.

Jin, P., Wang, T., Liu, N., Dupont, S., Beardall, J., and Boyd, P. W., et al.: Ocean acidification increases the accumulation of toxic phenolic compounds across trophic levels, Nat Commun., **6**, 8714. doi: 10.1038/ncomms9714, 2015.

Jin, P., Ding, J., Xing, T., Riebesell, U., & Gao, K.: High levels of solar radiation offset impacts of ocean acidification on calcifying and non-calcifying strains of *Emiliania huxleyi*, Mar. Ecol. Prog. Ser., **568**, 47-58. doi: 10.3354/meps12042, 2017.

Kirst, G. O.: Salinity Tolerance of Eukaryotic Marine Algae. Annu. Rev. Plant Physiol. Plant Mol. Biol., **41**, 21-53, doi: 10.1146/annurev.pp.41.060190.000321, 1990.

Langer, G., Nehrke, G., Probert, I., Ly, J., and Ziveri, P.: Strain-specific responses of *Emiliania huxleyi* to changing seawater carbonate chemistry. Biogeosciences **6**, 2637-2646, doi: 10.5194/bg-6-2637-2009, 2009.

LaRoche, J., Rost, B., and Engel, A.: Bioassays, batch culture and chemostat experimentation. In *Approaches and tools to manipulate the carbonate chemistry., Guide to Best Practices for Ocean Acidification Research and Data Reporting.* Riebesell U., Fabry VJ, Hansson L., Gattuso J. P., 81-94, 2010.

Lewis, E., Wallace, D., and Allison, L. J.: *Program developed for CO_2 system calculations*. ORNL/CDIAC-105, Oak Ridge, Tennessee, U.S.: Carbon Dioxide Information Analysis Center, Oak Ridge National Laboratory, Department of Energy, 1998.

Li, G., Gao, K., Yuan, D., Zheng, Y., and Yang, G.: Relationship of photosynthetic carbon fixation with environmental changes in the Jiulong River estuary of the South China Sea, with special reference to the effects of solar UV radiation, Marine Pollut Bull., **62**, 1852-1858. doi: 10.1016/j.marpolbul.2011.02.050, 2011.

Li, F., Beardall, J., Collins, S., and Gao, K.: Decreased photosynthesis and growth

with reduced respiration in the model diatom *Phaeodactylum tricornutum* grown under elevated CO_2 over 1800 generations, Global Change Biol., **23**, 127-137. doi: 10.1111/gcb.13501, 2017.

Liu, N., Beardall, J., and Gao, K.: Elevated CO_2 and associated seawater chemistry do not benefit a model diatom grown with increased availability of light, Aquat Microb Ecol., **79**, 137-147. doi: 10.3354/ame01820, 2017.

Lohbeck, K. T., Riebesell, U., and Reusch, T. B. H.: Adaptive evolution of a key phytoplankton species to ocean acidification, Nat Geosci., **5**, 346-351. doi: 10.1038/ngeo1441, 2012.

Mackinder, L., Wheeler, G., Schroeder, D., Riebesell, U., and Brownlee, C.: Molecular mechanisms underlying calcification in coccolithophores, Geomicrobiol. J., **27**, 585-595. doi: 10.1080/01490451003703014, 2010.

Massom, R. A., and Stammerjohn, S. E.: Antarctic sea ice change and variability – Physical and ecological implications, Polar Sci., **4**, 149-186, doi : 10.1016/j.polar.2010.05.001, 2010.

Monteiro, F. M., Bach, L. T., Brownlee, C., Bown, P., Rickaby, R. E., Poulton, A. J., et al: Why marine phytoplankton calcify, Sci. Adv., 2(7), e1501822, doi: 10.1126/sciadv.1501822, 2016.

Moore, T. S., Dowell, M. D., & Franz, B. A.: Detection of coccolithophore blooms in ocean color satellite imagery: A generalized approach for use with multiple sensors, Remote Sens of Environ., **117**, 249-263, doi: 10.1016/j.rse.2011.10.001, 2012.

678 Mork, M.: Circulation Phenomena and Frontal Dynamics of the Norwegian coastal
679 current, Philos. Trans. R. Soc., London **302**, 635-647, doi:
680 10.1098/rsta.1981.0188, 1981.
681 Müller, M., Schulz, K., and Riebesell, U.: Effects of long-term high CO_2 exposure on
682 two species of coccolithophores, Biogeosciences **7**, 1109-1116. doi:
683 10.5194/bg-7-1109-2010, 2010.
684 Nimer, N. A., and Merrett, M. J.: Calcification and utilization of inorganic carbon by
685 the coccolithophorid *Emiliania huxleyi* Lohmann, New Phytol., **121**, 173-177,
686 doi: 10.1111/j.1469-8137.1992.tb01102.x, 1992.
687 Nimer, N. A., and Merrett, M. J.: Calcification rate in *Emiliania huxleyi* Lohmann in
688 response to light, nitrate and availability of inorganic carbon, New Phytol., **123**,
689 673-677. doi : 10.1111/j.1469-8137.1993.tb03776.x, 1993.
690 Nimer, N. A., Brownlee, C., and Merrett, M. J.: Carbon dioxide availability,
691 intracellular pH and growth rate of the coccolithophore *Emiliania huxleyi*, Mar.
692 Ecol. Prog., **109**, 257-262. doi: 10.3354/meps109257, 1994.
693 O'Connor, B. S., Muller-Karger, F. E., Nero, R. W., Hu, C., and Peebles, E. B.: The
694 role of Mississippi River discharge in offshore phytoplankton blooming in the
695 northeastern Gulf of Mexico during August 2010, Remote Sens Environ., **173**,
696 133-144, doi: 10.1016/j.rse.2015.11.004, 2016.
697 Paasche, E.: The Adaptation of the Carbon‐14 Method for the Measurement of
698 Coccolith Production in *Coccolithus huxleyi*, Physiol. Plant., **16**, 186-200. doi:
699 10.1111/j.1399-3054.1963.tb08302.x, 1963.

700 Paasche, E., Brubak, S., Skattebøl, S., Young, J. R., and Green, J. C.: Growth and
701 calcification in the coccolithophorid *Emiliania huxleyi* (Haptophyceae) at low
702 salinities, Phycologia., **35**, 394-403. doi: 10.2216/i0031-8884-35-5-394.1, 1996.
703 Paasche, E.: A review of the coccolithophorid *Emiliania huxleyi* (Prymnesiophyceae),
704 with particular reference to growth, coccolith formation, and
705 calcification-photosynthesis interactions, Phycologia., **40**, 503-529, doi:
706 10.2216/i0031-8884-40-6-503.1, 2001.
707 Poulton, A. J., Adey, T. R., Balch, W. M., and Holligan, P. M.: Relating
708 coccolithophore calcification rates to phytoplankton community dynamics:
709 Regional differences and implications for carbon export, Deep-Sea Res. II, **54**,
710 538-557. doi: 10.1016/j.dsr2.2006.12.003, 2007.
711 Qi, D., Chen, L., Chen, B., Gao, Z., Zhong, W., and Feely, R. A., et al.: Increase in
712 acidifying water in the western Arctic ocean. Nat Clim Change, **7**, 195-199. doi:
713 10.1038/nclimate3228, 2017.
714 Raven, J., and Crawfurd, K.: Environmental controls on coccolithophore
715 calcification, Mar. Ecol. Prog., **470**, 137-166. doi: 10.3354/meps09993, 2012.
716 Ridgwell, A.: A Mid Mesozoic Revolution in the regulation of ocean chemistry. Mar.
717 Geol., **217**, 339-357, doi: 10.1016/j.margeo.2004.10.036, 2005.
718 Riebesell, U., Zondervan, I., Rost, B., Tortell, P. D., Zeebe, R. E., and Morel, F. M.:
719 Reduced calcification of marine plankton in response to increased atmospheric
720 CO_2, Nature **407**, 364-367, doi: 10.1038/35030078, 2000.
721 Riebesell, U., Bellerby, R. G., Engel, A., Fabry, V. J., Hutchins, D. A., Reusch, T. B.,

et al.: Comment on "Phytoplankton Calcification in a High-CO_2 World" , Science **322**, 1466, doi: 10.1126/science.1161096, 2008.

Ritchie, R. J.: Consistent sets of Spectrophotometric Chlorophyll Equations for Acetone, Methanol and Ethanol solvents, Photosynth Res., **89**, 27-41. doi: 10.1007/s11120-006-9065-9, 2006.

Rost, B., Riebesell, U., Burkhardt, S., and Sültemeyer, D.: Carbon acquisition of bloom‐forming marine phytoplankton. Limnol, Oceanogr., **48**, 55-67, doi: 10.4319/lo.2003.48.1.0055, 2003.

Rost, B., and Riebesell, U.: Coccolithophores and the biological pump: responses to environmental changes, In Thierstein HR, Young JR (eds), *Coccolithophores—From Molecular Processes to Global Impact*, Berlin: Springer 76-99, 2004.

Sabine, C. L., Feely, R. A., Gruber, N., Key, R. M., Lee, K., and Bullister, J. L., et al.: The Oceanic Sink for Anthropogenic CO_2, Science **305**, 367-371. doi: 10.1126/science.1097403, 2004.

Saruwatari, K., Satoh, M., Harada, N., Suzuki, I., and Shiraiwa, Y.: Change in coccolith morphology by responding to temperature and salinity in coccolithophore *Emiliania huxleyi* (Haptophyta) isolated from the Bering and Chukchi seas, Biogeosci Discuss., **12**, 17751-17780, doi: 10.5194/bgd-12-17751-201, 2015.

Schouten, S., Ossebaar, J., Schreiber, K., Kienhuis, M. V. M., Langer, G., and Benthien, A., et al.: The effect of temperature, salinity and growth rate on the

744 stable hydrogen isotopic composition of long chain alkenones produced by
745 *Emiliania huxleyi* and *Gephyrocapsa oceanica*. Biogeosci Discuss., **2**,
746 1681-1695, doi: 10.5194/bg-3-113-2006, 2006.
747 Schulz, K. G., Rost, B., Burkhardt, S., Riebesell, U., Thoms, S., and Wolf-Gladrow, D.
748 A.: The effect of iron availability on the regulation of inorganic carbon
749 acquisition in the coccolithophore *Emiliania huxleyi* and the significance of
750 cellular compartmentation for stable carbon isotope fractionation. Geochim,
751 Cosmochim, Acta **71**, 5301-5312. doi: 10.1016/j.gca.2007.09.012, 2007.
752 Sekino, K., and Shiraiwa, Y.: Accumulation and utilization of dissolved inorganic
753 carbon by a marine unicellular coccolithophorid, *Emiliania huxleyi*, Plant
754 Physiol., **35**, 353-361. doi: 10.1093/oxfordjournals.pcp.a078603, 1994.
755 Sett, S., Bach, L. T., Kai, G. S., Kochklavsen, S., Lebrato, M., & Riebesell, U.:
756 Temperature modulates coccolithophorid sensitivity of growth, photosynthesis
757 and calcification to increasing seawater pCO_2, Plos One **9**, e88308, doi:
758 10.1371/journal.pone.0088308, 2014.
759 Shi, D., Xu, Y., and Morel, F. M. M.: Effects of the pH/pCO_2 control method on
760 medium chemistry and phytoplankton growth, Biogeosciences **6**, 1199-1207.
761 doi: 10.5194/bg-6-1199-2009, 2009.
762 Sikes, C. S., and Wilbur, K. M.: Functions of coccolith formation, Limnol. Oceanogr.,
763 **27**, 18-26. doi: 10.4319/lo.1982.27.1.0018, 1982.
764 Stojkovic, S., Beardall, J., and Matear, R.: CO_2-concentrating mechanisms in three
765 southern hemisphere strains of *Emiliania huxleyi*, J. Phycol., **49**, 670-679, doi:

766 10.1111/jpy.12074, 2013.

767 Strickland, J. D. H., and Parsons, T. R.: A practical handbook of seawater
768 analysis. *Bulletin, 167,*1972.

769 Suffrian, K., Schulz, K. G., Gutowska, M. A., Riebesell, U., and Bleich, M.: Cellular
770 pH measurements in *Emiliania huxleyi* reveal pronounced membrane proton
771 permeability, New Phytol., **190**, 595-608, doi:
772 10.1111/j.1469-8137.2010.03633.x, 2011.

773 Sunda, W. G., Price, N. M., and Morel, F. M.: Trace metal ion buffers and their use in
774 culture studies, in *Algal culturing techniques*, Robert A. Andersen (Academic
775 Press), **4**, 35-63, 2005.

776 Taucher, J., & Oschlies, A.: Can we predict the direction of marine primary
777 production change under global warming? Geophys. Res. Lett., **38**, 104-113. doi:
778 10.1029/2010GL045934, 2011.

779 Taylor, A. R., Chrachri, A., Wheeler, G., Goddard, H., & Brownlee, C.: A
780 Voltage-Gated H^+ Channel Underlying pH Homeostasis in Calcifying
781 Coccolithophores, Plos Biology **9**, e1001085, doi: 10.1371/journal.pbio.1001085,
782 2011.

783 Tyrrell, T., Schneider, B., Charalampopoulou, A., and Riebesell, U.: Coccolithophores
784 and calcite saturation state in the Baltic and Black seas, Biogeosciences, **5**,
785 485-494. doi: 10.5194/bgd-4-3581-2007, 2007.

786 Wal, P. V. D., Kempers, R. S., and Veldhuis, M.: Production and downward flux of
787 organic matter and calcite in a North sea bloom of the coccolithophore *Emiliania*

huxleyi, Mar. Ecol. Prog., **126**, 247-265. doi: 10.3354/meps126247, 1995.

Werdan, K., Heldt, H. W., and Milovancev, M: The role of pH in the regulation of carbon fixation in the chloroplast stroma. Studies on CO_2 fixation in the light and dark, Biochim. Biophys. Acta **396**, 276-292, doi: 10.1016/0005-2728(75)90041-9, 1975.

Winter, A., Jordan, R. W., and Roth, P. H.: "*Biogeography of coccolithophores in ocean waters*," in *Coccolithophores*. Amos Winter and William G. Siesser (eds) , Cambridge University Press, UK, p161-177, 1994.

Wulff, A., Karlberg, M., Olofsson, M., Torstensson, A., Riemann, L., and Steinhoff, F., et al.: Climate-driven change in a Baltic sea summer microplanktonic community – desalination play a more important role than ocean acidification, Biogeosci Discuss., 1-32, doi: 10.5194/bg-2016-383, 2016.

Xu, K., and Gao, K.: Reduced calcification decreases photoprotective capability in the coccolithophorid *Emiliania huxleyi*, Plant Physiol., **53**, 1267-1274, doi: 10.1093/pcp/pcs066, 2012.

Zondervan, I., Rost, B., and Riebesell, U.: Effect of CO_2 concentration on the PIC/POC ratio in the coccolithophore *Emiliania huxleyi* grown under light-limiting conditions and different daylengths, J. Exp. Mar. Biol. Ecol., **272**, 55-70, doi: 10.1016/S0022-0981(02)00037-0, 2002

Biogeosciences Discuss., https://doi.org/10.5194/bg-2019-4
Manuscript under review for journal Biogeosciences
Discussion started: 15 February 2019

807 **Figure captions**

808 Figure 1. Specific growth rates (a) and cell diameters (b) of *Emiliania huxleyi* at three
809 salinities (LC, open circles; HC, solid squares). The dashed line is the linear
810 regression result of the growth rates under LC (y= -0.01142x + 1.43055, R^2 = 0.88).
811 Values are means ± SD of triplicate cultures. Symbols with different lowercase letters
812 indicate significant differences ($p < 0.05$) among different treatments.

813

814 Figure 2. Chl *a* (a), Chl *c* (b) and Carotenoids (c) contents of *Emiliania huxleyi* at
815 three salinities (LC, open circles; HC, solid squares). Two dashed lines are the linear
816 regression results of the chlorophyll *a* and carotenoids contents under HC respectively.
817 (y= -0.00562x + 0.23105, R^2 = 0.94; y= -0.00681x + 0.28755, R^2 = 0.99). Values are
818 means ± SD of triplicate cultures. Symbols with different lowercase letters indicate
819 significant differences ($p < 0.05$) among different treatments.

820

821 Figure 3. Maximum (a) and effective photochemical quantum yields (b) of *Emiliania*
822 *huxleyi* at three salinities (LC, open circles; HC, solid squares). Values are means ±
823 SD of triplicate cultures. Symbols with different lowercase letters indicate significant
824 differences ($p < 0.05$) among different treatments.

825

826 Figure 4. Photosynthetic rates (a), calcification rates (b) at 6 h after the onset of light
827 and calcification to photosynthesis ratio—C: P (c) of three salinities (LC, open circles;
828 HC, solid squares). The dash-dotted line and solid line are the linear regression results

of the photosynthetic rates under LC and HC, respectively (y= -0.03624x + 1.49612, R^2 = 0.89; y= -0.03173x + 1.22979, R^2 = 0.99). Values are means ± SD of triplicate cultures. Symbols with different lowercase letters indicate significant differences (p < 0.05) among different treatments.

Figure 5. Changes in effective photochemical quantum yield of cells grown under ambient (400 µatm, LC, a) and elevated CO_2 (1000 µatm, HC, b) when exposed to solar radiation for 48 min (800 µmol photons m^{-2} s^{-1}) under three salinity treatments: 25‰ (open triangles), 30‰ (half solid circles) and 35‰ (solid squares). Values are means ± SD of triplicate cultures. Asterisks represent significant differences (p < 0.05) among three salinity treatments.

Figure 6. Rate of Repair r (a), damage k (b) and the ratio of repair:damage (c) after exposure to solar radiation for 48 min (800 µmol photons m^{-2} s^{-1}) under different treatments (LC, open circles; HC, solid squares). Values are means ± SD of triplicate cultures. Symbols with different lowercase letters indicate significant differences (p < 0.05) among different treatment

Biogeosciences Discuss., https://doi.org/10.5194/bg-2019-4
Manuscript under review for journal Biogeosciences
Discussion started: 15 February 2019

Table 1. Carbonate chemistry parameters of culture media before inoculation (already equilibrated with the ambient or elevated CO_2 levels). Values are means ± SD of triplicate cultures.

Treatment	PH_{NBS}	TA ($\mu mol\ kg^{-1}$)	DIC ($\mu mol\ kg^{-1}$)	HCO_3^- ($\mu mol\ kg^{-1}$)	CO_3^{2-} ($\mu mol\ kg^{-1}$)	CO_2 ($\mu mol\ kg^{-1}$)	pCO_2 (ppm)
25‰ LC	8.01 ± 0.01	1480.25 ± 8.64	1361.07 ± 10.20	1274.62 ± 10.50	74.20 ± 0.60	12.21 ± 0.30	388.24 ± 9.44
25‰ HC	7.61 ± 0.01	1510.52 ± 23.74	1479.59 ± 25.15	1412.84 ± 24.02	33.52 ± 0.02	33.23 ± 1.11	1035.84 ± 33.97
30‰ LC	8.07 ± 0.01	1735.08 ± 8.33	1555.20 ± 10.48	1432.15 ± 11.16	112.05 ± 0.95	11.00 ± 0.26	360.24 ± 8.62
30‰ HC	7.68 ± 0.01	1787.40 ± 19.06	1725.08 ± 20.63	1641.80 ± 19.97	52.33 ± 0.21	30.95 ± 0.88	998.16 ± 27.98
35‰ LC	8.09 ± 0.01	1977.95 ± 0.64	1749.50 ± 3.86	1594.03 ± 5.49	144.05 ± 1.85	11.42 ± 0.22	384.45 ± 7.53
35‰ HC	7.71 ± 0.01	2019.13 ± 0.66	1931.75 ± 2.83	1831.30 ± 3.26	68.99 ± 1.00	31.46 ± 0.57	1045.53 ± 18.49

851 Table 2. Carbonate chemistry parameters of culture media on the last day of incubation. Values are means ± SD of triplicate cultures.

Treatment	PH_{NBS}	TA (µmol kg^{-1})	DIC (µmol kg^{-1})	HCO_3^- (µmol kg^{-1})	CO_3^{2-} (µmol kg^{-1})	CO_2 (µmol kg^{-1})
25‰ LC	7.80 ± 0.02	1431.04 ± 87.94	1362.03 ± 81.89	1294.78 ± 76.69	47.55 ± 4.96	19.70 ± 0.27
25‰ HC	7.64 ± 0.02	1487.42 ± 15.34	1451.53 ± 15.54	1385.89 ± 14.87	34.85 ± 1.38	30.79 ± 1.32
30‰ LC	7.96 ± 0.01	1704.14 ± 107.22	1564.82 ± 99.62	1461.77 ± 91.74	88.54 ± 7.72	14.51 ± 0.80
30‰ HC	7.65 ± 0.02	1743.80 ± 21.78	1691.49 ± 27.10	1611.22 ± 26.52	47.04 ± 2.01	33.23 ± 2.44
35‰ LC	8.00 ± 0.07	1969.47 ± 7.73	1775.25 ± 21.29	1636.87 ± 35.54	124.21 ± 16.66	14.18 ± 2.39
35‰ HC	7.72 ± 0.01	2002.71 ± 3.20	1909.95 ± 7.89	1809.04 ± 8.87	71.11 ± 2.16	29.81 ± 1.19

852

853

854

Biogeosciences Discuss., https://doi.org/10.5194/bg-2019-4
Manuscript under review for journal Biogeosciences
Discussion started: 15 February 2019

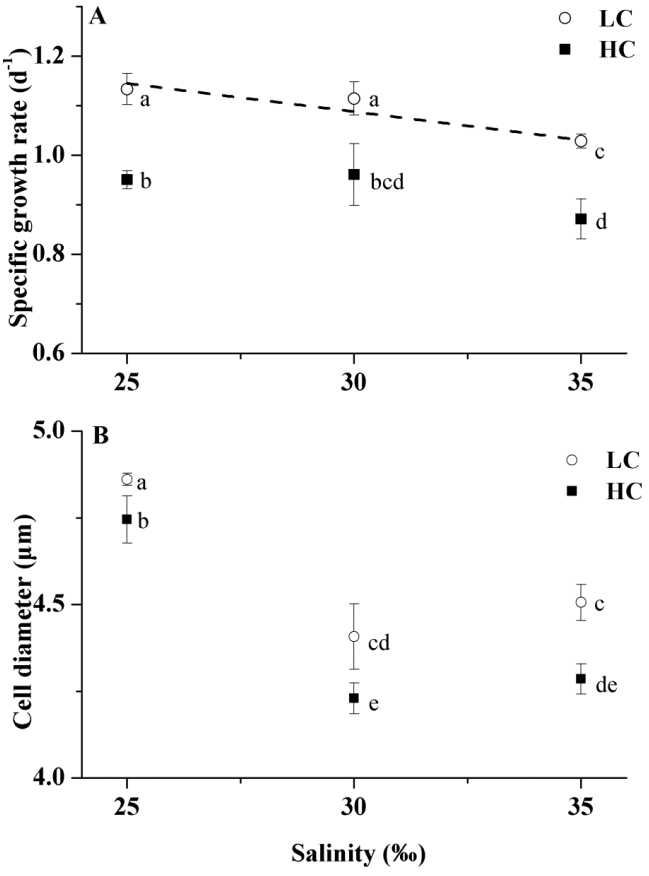

Biogeosciences Discuss., https://doi.org/10.5194/bg-2019-4
Manuscript under review for journal Biogeosciences
Discussion started: 15 February 2019

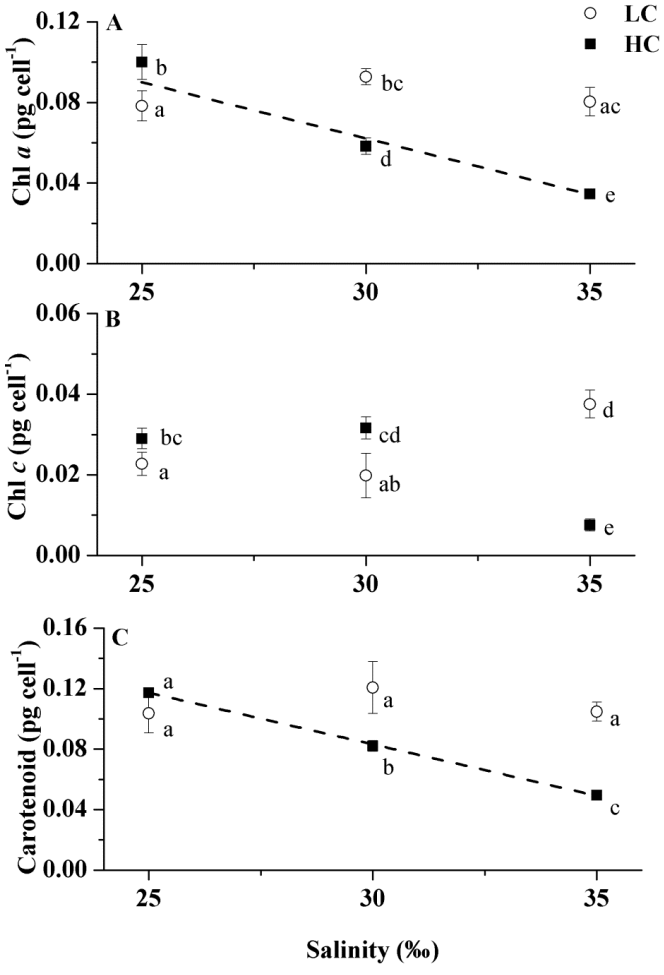

Biogeosciences Discuss., https://doi.org/10.5194/bg-2019-4
Manuscript under review for journal Biogeosciences
Discussion started: 15 February 2019

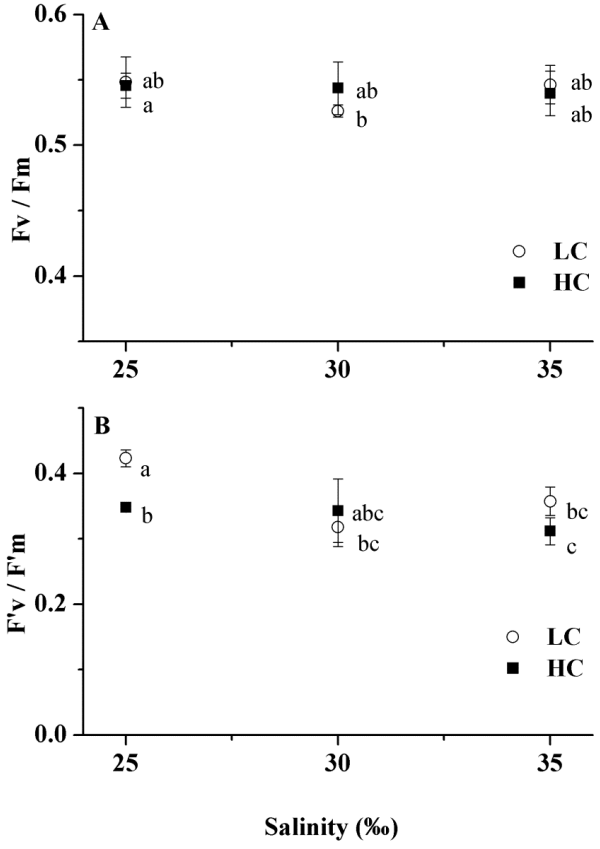

Biogeosciences Discuss., https://doi.org/10.5194/bg-2019-4
Manuscript under review for journal Biogeosciences
Discussion started: 15 February 2019

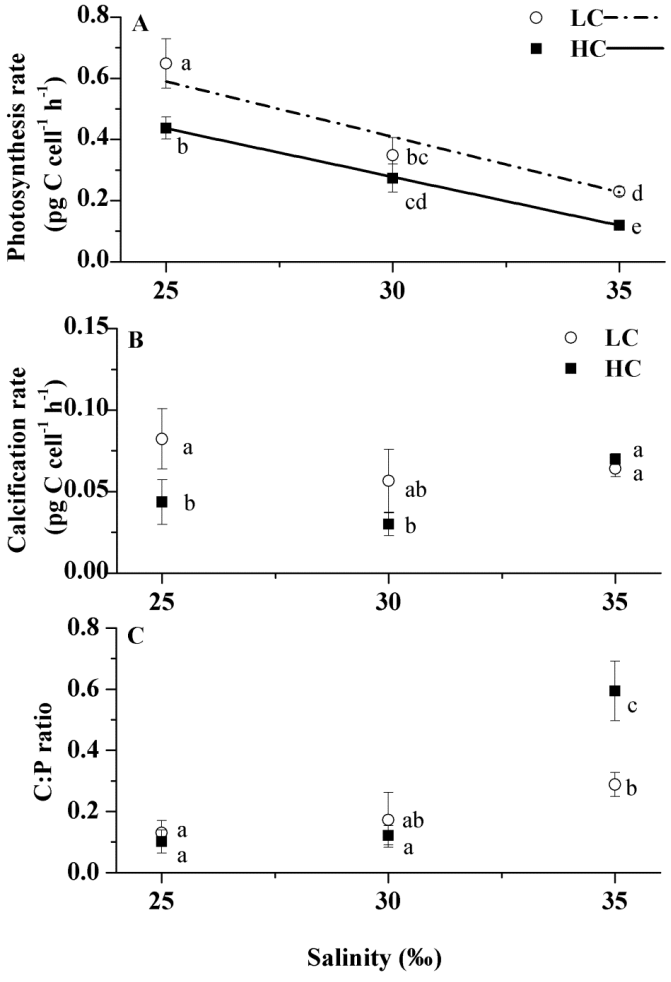

Biogeosciences Discuss., https://doi.org/10.5194/bg-2019-4
Manuscript under review for journal Biogeosciences
Discussion started: 15 February 2019

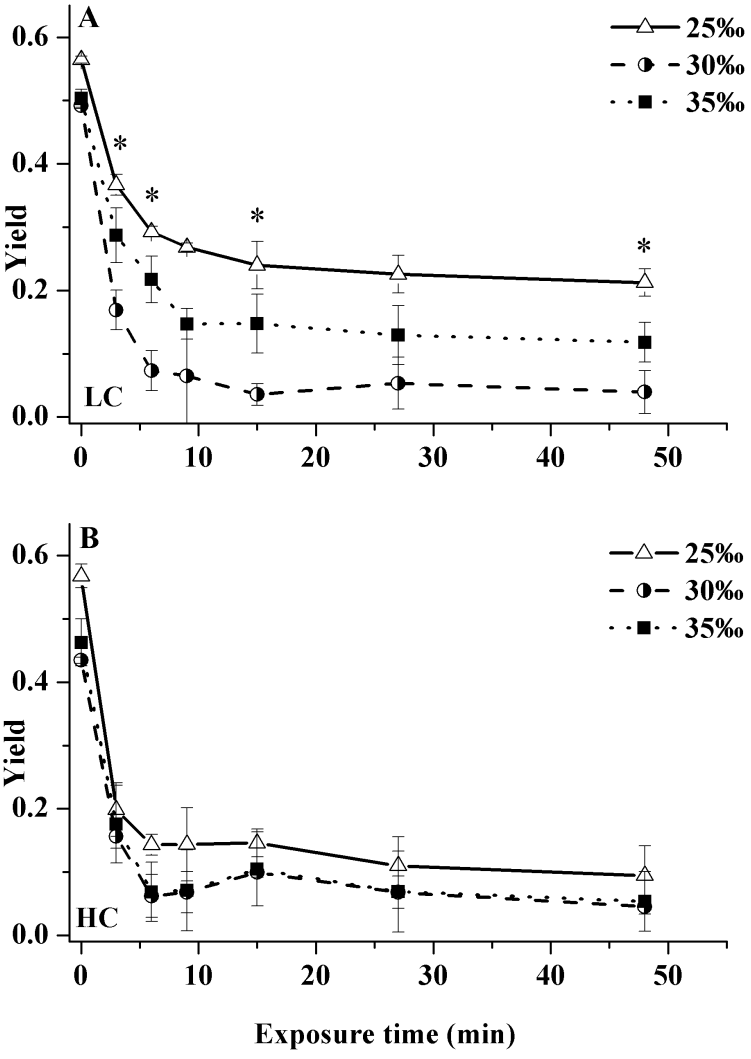

Biogeosciences Discuss., https://doi.org/10.5194/bg-2019-4
Manuscript under review for journal Biogeosciences
Discussion started: 15 February 2019